Anomalous free energy changes induced by topology

Ying Tang,[1,2,*] Ruoshi Yuan,[3,†] and Ping Ao[1,2,‡]

[1]*Department of Physics and Astronomy, Shanghai Jiao Tong University, Shanghai 200240, China*

[2]*Key Laboratory of Systems Biomedicine Ministry of Education, Shanghai Center for Systems Biomedicine, Shanghai Jiao Tong University, Shanghai 200240, China*

[3]*School of Biomedical Engineering, Shanghai Jiao Tong University, Shanghai 200240, China*

(Received 16 June 2015; revised manuscript received 28 October 2015; published 16 December 2015)

We report that nontrivial topology of a driven Brownian particle restricted on a ring leads to anomalous behaviors on free energy change. Starting from steady states with identical distribution and current on the ring, free energy changes are distinct and nonperiodic after the system is driven by the same periodic force protocol. We demonstrate our observation in examples through both exact solutions and numerical simulations. The free energy calculated here can be measured in recent experimental systems.

DOI: 10.1103/PhysRevE.92.062129 PACS number(s): 05.70.Ln, 05.10.Gg, 05.40.−a

I. INTRODUCTION

Thermodynamics plays a crucial role in understanding chemical and biophysical processes [1]. These systems are usually out of equilibrium with breakdown of detailed balance, which has intricacy in discussing fundamental thermodynamical quantities inherited from equilibrium case. A typical example is a Brownian particle on a ring subject to a conservative periodic potential and a nonconservative time-dependent force $f(t)$ [2–5], as shown in Fig. 1. One intriguing property of this system is the nontrivial topology: the dynamics is invariant under rotational transformation on the angular variable $\theta \to \theta + 2\pi$, and such topological space allows a persistent current breaking detailed balance at the steady state. In this paper, we report that the nontrivial topology leads to anomalous behaviors on free energy change even for a primitive model of a realistic experimental system with a Brownian particle on a ring [3,4]. Specifically, starting from steady states with identical distribution and current on the ring, free energy changes are distinct even when the system is driven by the same periodic force afterwards. Our observation demonstrates that these steady states are degenerated when observed on the ring, and they indeed have different actual distributions, which can be revealed by considering the particle moving along a tilted potential. For this potential, giant acceleration of the effective diffusion has been observed both theoretically [6,7] and experimentally [3,8,9]. Our present result then uncovers another anomalous phenomenon on thermodynamics of such stochastic dynamics with the tilted potential, and free energy changes calculated here can be measured in real experiments to distinguish the degenerated steady states.

The stochastic dynamics on a ring serves as a paradigm to recent studies on fluctuation theorems [2,3,10–12] and generalized fluctuation-dissipation relations [3,4,13]. The total entropy production in the fluctuation theorem can be expressed in terms of work and free energy only when the driven system is initially at (canonical) equilibrium. Since the canonical ensemble is absent for the nonequilibrium system on a ring, how to quantify free energy change between steady states corresponding to the work conducted is still unclear. Consider a straightforward case with flat potential. The particle will relax to steady states that all have a uniform distribution on the ring regardless of the varying force $f(t)$ [5]. As a result, the steady state distribution does not provide information on the free energy change. In the following, we will demonstrate in detail how to extract free energy changes for such dynamics and then apply our methods to experimentally realizable examples. Our method extends theoretically the concept of free energy to nonequilibrium steady states by an exact and unique definition, which needs to be tested by experiments.

This paper is organized as follows. In Sec. II we provide the method to calculate free energy change and discuss briefly its anomalous behaviors. In Sec. III we use both analytic calculation and numerical simulation to obtain free energy in two examples and present the detailed analysis on the behavior of free energy change. We then discuss our results in Sec. IV. In Sec. V we summarize our work. In the Appendices we provide the details for the calculations and simulations for the two examples.

II. THE STOCHASTIC DYNAMICS

We start from the stochastic dynamics on a ring described by the Langevin equation:

$$\dot{\theta} = -D\partial_\theta V(\theta) + f(t) + \sqrt{2D}\xi(t), \tag{1}$$

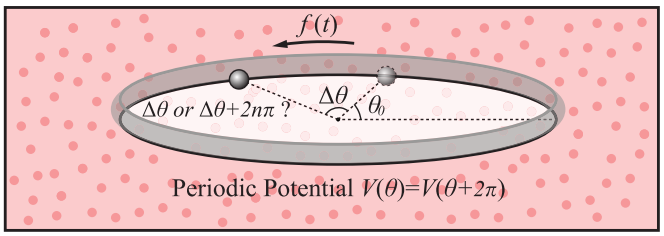

FIG. 1. (Color online) An illustrative picture of a Brownian particle on the ring described by Eq. (1). When observing the particle on the ring, the paths with displacement $\Delta\theta$ include degenerated path configurations with $\Delta\theta + 2n\pi$, where $n \in \mathcal{Z}$ denotes winding number.

*jamestang23@gmail.com
†rsyuan.acm06@gmail.com
‡aoping@sjtu.edu.cn

where $\theta \in [0,2\pi)$ denotes the angular variable on the ring, D is the diffusion constant, $\xi(t)$ is a Gaussian white noise modeling the thermal bath with $\langle \xi(t) \rangle = 0$, $\langle \xi(t)\xi(s) \rangle = \delta(t-s)$, and temperature T is set as unit. The time-dependent control parameter $f(t)$ denotes a nonconservative force. Here the conservative potential function satisfies the periodic boundary condition: $V(\theta) = V(\theta + 2\pi)$, which guarantees the rotational symmetry of the dynamics on the ring. We have assumed that the Einstein relation $D = T\mu$ holds in the nonequilibrium situation [3], where μ is the mobility constant. We have also used the overdamped approximation, and the case with inertial term can be discussed without essential difficulty. Equation (1) can be applied to model a wide class of systems, including the Brownian motor [14], the rotary motor protein [15], and the Josephson junction [16,17].

A. Construction on tilted potential

A time-dependent potential function [18] is constructed with its gradient as the total drift force:

$$\phi[\theta, f(t)] = V(\theta) - \frac{1}{D} f(t)\theta, \tag{2}$$

and Eq. (1) can be rewritten as $\dot{\theta} = -D\partial_\theta \phi[\theta, f(t)] + \sqrt{2D}\xi(t)$. Note that $\phi[\theta, f(t)] \neq \phi[\theta + 2\pi, f(t)]$, and thus the particle is treated as moving in a tilted potential. The steady state of Eq. (1) is typically not given by the Boltzmann-Gibbs distribution $\exp(-\phi)/Z$ [or $\exp(-V)/Z$] [19], where Z is the partition function.

When driven by the force, the particle has different states when it completes one more circle on the ring, i.e., the states with different winding numbers are distinct. This property can be revealed by considering the particle moving along this tilted potential [5,20]. With using the tilted potential, the ring is mapped into real line $\mathcal{R}$. Starting from an initial distribution on $[0,2\pi)$, the ensemble distribution of the particle flows outside $[0,2\pi)$ to $(-\infty, +\infty)$. The states of the system are determined by the actual ensemble distribution on the line. When observed on the ring, there can be degenerated states with the same distribution and current, and their actual ensemble distributions on real line are distinct (see Sec. III).

B. Free energy

In this subsection, we provide the procedure to extract free energy. In our previous work, we have generalized the free energy [21,22] to nonequilibrium steady states of stochastic dynamics with natural boundary condition. To our knowledge, the concept of free energy for nonequilibrium steady states of Eq. (1) with periodic boundary condition has not been established before. Our method here is to extend Jarzynski's method [23] to quantify free energy. We define the free energy by the ensemble average of the work conducted in Eq. (7). This ensemble average quantifies the energy change due to the work performed and can be obtained through measuring the work ensemble in experiments [24]. The present definition on free energy is consistent with that by the canonical partition function for system without nontrivial topology. For quantum systems with periodic boundary condition [25], further generalization on free energy definition is needed.

To calculate the ensemble average, we should count the path degeneracy caused by the topological property of the ring: the angular variables θ of the Brownian motion on the ring with different winding numbers are indistinguishable due to the rotational symmetry. Therefore, we construct an ensemble that counts paths with all winding numbers:

$$\langle e^{-A} \rangle_{\mathrm{PD}} = \int_0^{2\pi} d\theta_N \sum_{m=-\infty}^{\infty} \int_0^{2\pi} d\theta_0 P_{ss}(\theta_0, t_0) \times P_A^m(\theta_N t_N | \theta_0 t_0), \tag{3}$$

where A is a thermodynamical variable along a path, and $P_A^m(\theta_N t_N|\theta_0 t_0) \doteq P^m(\theta_N t_N|\theta_0 t_0)e^{-A}$. The initial state is assumed to obey the steady state distribution $P_{ss}(\theta_0, t_0)$. Here the weighted transition probability $P_A^m(\theta_N t_N|\theta_0 t_0)$ is calculated by employing the path integral in the winding number representation [20], where m denotes the winding number, and $\langle \cdots \rangle_{\mathrm{PD}}$ means the ensemble average with path degeneracy (PD). For each m, the path integral is [26,27]

$$P^m(\theta_N t_N|\theta_0 t_0) = \int_{\theta_0}^{\theta_N + 2\pi m} \mathcal{D}\theta \exp - \int_{t_0}^{t_N} \times \left[\frac{1}{4D}(\dot{\theta} + D\partial_\theta \phi)^2 - \frac{1}{2}\frac{d(D\partial_\theta \phi)}{d\theta} \right] dt, \tag{4}$$

with $\int_{\theta_0}^{\theta_N + 2\pi m} \mathcal{D}\theta \doteq \lim_{N\to\infty} \frac{1}{\sqrt{2\pi\tau\epsilon}} \prod_{n=1}^{N-1} \int_{-\infty}^{\infty} \frac{d\theta_n}{\sqrt{2\pi\tau\epsilon}}$. Through a smooth map from the ring to the real line, we can do the path integration on the line with the point at time t_N being $\theta_N + 2\pi m$ for the paths of winding number m [20]. If θ_N goes one more complete circle, P^m becomes P^{m+1} while the ensemble average of work in the main text has to show no physical change, and thus the prefactor of P^m is unity for all m. Note that the integral of the action function on the exponent obeys ordinary calculus, because we employ the Stratonovich interpretation and thus the prefactor of the Jacobian term is $1/2$ [27].

We use the definition of work for a single path [22,23,28] as variation of the time-dependent potential with respect to all the control parameters:

$$W = \int_{t_0}^{t_N} dt\, \dot{f} \frac{\partial \phi}{\partial f}. \tag{5}$$

Then the ensemble average for the work with counting all winding numbers $\langle e^{-W} \rangle_{\mathrm{PD}}$ is given by Eq. (3) with weighted path integral of winding number m:

$$P_W^m(\theta_N t_N|\theta_0 t_0) = P^m(\theta_N t_N|\theta_0 t_0) e^{-\int_{t_0}^{t_N} dt\, \dot{f}(\partial\phi/\partial f)}. \tag{6}$$

Free energy change is

$$\Delta \mathcal{F} = -\ln \langle e^{-W} \rangle_{\mathrm{PD}}. \tag{7}$$

When the control parameter stops varying and becomes a nonzero constant afterwards, the system will finally relax to a nonequilibrium steady state. As $\dot{f} = 0$ in the process of relaxation, the free energy does not change during this period. When driven by the force, the particle on the ring has different

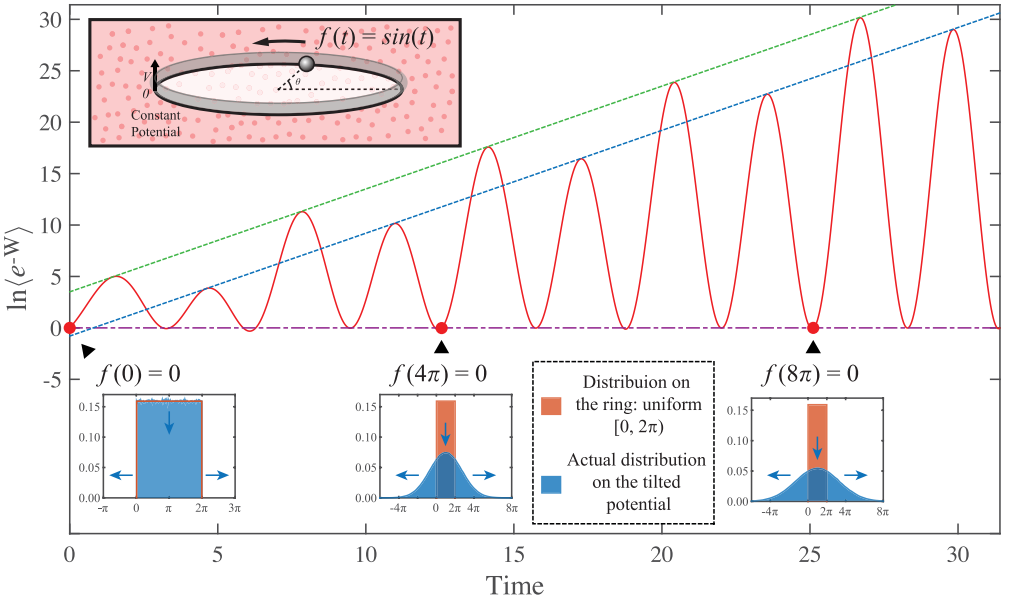

FIG. 2. (Color online) Free energy changes of Eq. (8) with $f(t) = \sin \omega t$. The ensemble distributions observed on the ring at time $t = 0, 4\pi, 8\pi$ are all uniform, with the same free energy and current (degenerated states). Their actual distributions along the tilted potential on real line are different, and free energy changes afterwards are distinct. The slopes of the dashed lines connecting alternate peaks are the same from Eq. (12). The parameters are $t_0 = 0$, $D = \omega = 1$.

states when it completes one more circle. Therefore, winding numbers should be taken as an additional state variable. Then the free energy definition is unique for the nonequilibrium steady state with a specific winding number.

The distinct actual ensemble distributions of the degenerated states with the same distribution and current observed on the ring lead to different free energy changes even when driven by the same force protocol. Take Eq. (8) below as an example: the steady state distribution observed on the ring is always uniform, and there are different states all with zero current (force), as shown in Fig. 2. Starting from these degenerated states, free energy changes are distinct even under the same periodic force $f(t) = \sin \omega t$, and the maximum of free energy is enhanced after each 2π period. On the other hand, free energy change calculated by Eq. (7) under periodic force does not show such anomalous behaviors for systems without nontrivial topology [22,23,29], where the variation of free energy under periodic force is typically periodic.

Originally, Jarzynski equality connects the free energy difference between equilibriums and the work of nonequilibrium process: $\langle e^{-W} \rangle_{\text{path}} = e^{-\Delta \mathcal{F}}$ [23,24,30,31]. It could not be applied directly to the present dynamics with nontrivial topology: due to the breakdown of detailed balance, the free energy in Jarzynski equality can no longer be generally defined by the equilibrium canonical ensemble. Here, as an alternative treatment of Jarzynski, we define free energy difference between steady states through calculating $\langle e^{-W} \rangle_{\text{PD}}$. Our method agrees with that of Jarzynski for systems without nontrivial topology and extends the free energy definition in a consistent manner to systems with nontrivial topology. This free energy corresponds to the work conducted, and can also be measured experimentally to distinguish the degenerated steady states with the same distribution and current observed on the ring (see Sec. IV).

III. FREE ENERGY CALCULATION IN EXAMPLES

A. First example

We next calculate free energy change in two examples. The first has a flat conservative potential:

$$\dot{\theta} = f(t) + \sqrt{2D}\xi(t). \tag{8}$$

The time-dependent potential function is $\phi[\theta, f(t)] = -f(t)\theta/D$. The steady state with distribution P_{ss} has a current $J_{ss} = f(t)P_{ss}$ and its average $\langle \dot{\theta} \rangle_{ss} = f(t)$. By solving the path integral with choosing the initial distribution $P_{ss}(\theta_0, t_0) = \delta(\theta - \theta_0)$ in Appendix A, we obtain the transition probability $P(\theta_N t_N | t_0) = \theta_3\{[-\theta_N + \int_{t_0}^{t_N} f(t)\,dt\}/2, iD\Delta t/\pi]/2\pi \to 1/2\pi$ when $t_N \to \infty$, where θ_3 is the Jacobi theta function [32]. Note that the Hatano-Sasa relation [2] is straightforwardly satisfied in this example.

We consider the driving process that starts from a steady state distribution $P_{ss}(\theta_0, t_0)$ on $[0, 2\pi)$ and continues to time t_N. From the work formula [Eq. (5)], we have $W = -\int_{t_0}^{t_N} dt\, \dot{f}\theta/D$. With $P_{ss}(\theta_0, t_0) = 1/2\pi$, we obtain free energy by solving the path integral in Eq. (7):

$$-\Delta \mathcal{F} = \ln\left(\frac{D\{e^{2\pi[f(t_N)-f(t_0)]/D} - 1\}}{2\pi[f(t_N) - f(t_0)]}\right) + \frac{1}{D} f(t_N)\left[\Delta t f(t_N) - \int_{t_0}^{t_N} f\,dt\right]. \tag{9}$$

The detailed calculation is given in Appendix A. When $f(t)$ keeps constant, $-\Delta \mathcal{F} = 0$ as $W = 0$. When the control parameter varies, free energy changes, and current strength also varies leading to different steady states. Therefore, free energy quantifies the energy to drive the system from one steady state to another, consistent with that used to connect two equilibriums [23,24,30].

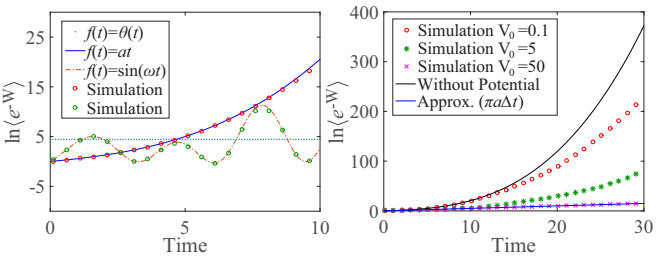

(a) Constant Potential (b) Cosine Potential

FIG. 3. (Color online) Free energy changes of Eq. (8) with different force protocols and Eq. (13) with linear force protocol. (a) The lines are plotted by the explicit formulas: (1) dotted line is $f(t) = \Delta f \theta(t)$, (2) dashed line is $f(t) = at$, (3) solid line is $f(t) = \sin \omega t$. The circles are simulations, which sample 300 000 paths. (b) The circles are simulation results with three different heights of the periodic potential: $V_0 = 0.1$, $V_0 = 5$, and $V_0 = 50$. Two approximations for sufficiently large and small potential height are plotted and match the simulations in specific time regions. More data can be viewed in the Appendices. The parameters are $t_0 = 0$, $D = \Delta f = \omega = k_0 = 1$, and $a = 0.16$.

We discuss different protocols of $f(t)$: (1) $f(t) = \Delta f \theta(t)$ with $\theta(t)$ as a step function, (2) $f(t) = at$, (3) $f(t) = \sin \omega t$, and we separately have free energy changes $-\Delta\mathcal{F}$:

$$\ln\{D(e^{2\pi \Delta f/D} - 1)/(2\pi \Delta f)\}, \tag{10}$$

$$\ln\{D\{e^{2\pi a \Delta t/D} - 1\}/(2\pi a \Delta t)\} + a^2 t_N \Delta t^2/2D, \tag{11}$$

$$\ln\{D[e^{2\pi(\sin \omega t_N - \sin \omega t_0)/D} - 1]/[2\pi(\sin \omega t_N - \sin \omega t_0)]\} + \sin \omega t_N[\Delta t \sin \omega t_N - (\cos \omega t_0 - \cos \omega t_N)/\omega]/D. \tag{12}$$

The detailed calculation is given in Appendix A. We also use simulation to sample $-\Delta\mathcal{F}$, and they match the explicit formulas well, as in Fig. 3. In addition, though we start from a steady state with zero current ($f(0) = 0$), our method [Eq. (6)] is applicable to cases with nonzero current initially by using the corresponding steady state distribution. We obtain results with various initial distributions in Appendix A.

Under the force $f(t) = \Delta f \theta(t)$, free energy suddenly changes from zero to a finite value as the system moves to another state. After the sudden jump of the force, the system relaxes to a steady state without further free energy change. Further anomalous behaviors happen with the continuously varying forces. For $f(t) = at$, we have different varying speeds with distinct a. Consider driving processes with the same final force strength $\Lambda = at_N$, then $-\Delta\mathcal{F} = \ln\{D[e^{2\pi\Lambda/D} - 1]/(2\pi\Lambda)\} + \Lambda^2 t_N/2D$. Note that for smaller a, t_N is larger to keep Λ constant, leading to a larger $-\Delta\mathcal{F}$. This says that even the final force strength is the same, free energy changes are different for distinct speeds of varying the linear force.

For $f(t) = \sin t$, when force is zero at $t = n\pi (n \in \mathcal{Z})$, free energy is zero, and the system has an uniform distribution on the ring. When force is nonzero, the system does not relax to an equilibrium but to a nonequilibrium steady state with current. The actual ensemble distribution of the particle on real line keeps changing due to the force and diffusion, and free energy changes can be different when the force protocols are the same. For example, the maximum of free energy is enhanced after each 2π period, as in Fig. 2, and the reason is as follows. The system starts from a uniform distribution on $[0,2\pi)$ and keeps diffusing. The value of $-\Delta\mathcal{F} = \ln\langle\exp(\int_{t_0}^{t_N} dt\, \dot{f}\theta/D)\rangle$ raises after a 2π period as shown in Eq. (12). Intuitively, the particle with larger θ value moves a longer distance, which needs more work to drive it there.

We also observe an "undershooting" behavior of free energy change with $f(t) = \sin t$, where free energy can be negative during each time period of π/ω as shown in Fig. 2. According to Eq. (9), when time approaches to $t = \pi/\omega$, $f(t) = \sin \omega t$ is positive, but $[\Delta t f(t_N) - \int_{t_0}^{t_N} f dt]$ can be negative, leading to negative free energy. This phenomenon is caused by the diffusion of the particle. Intuitively the particle keeps diffusing when dragged by the external force, and it requires more free energy when the force returns to zero than that when the force deviates from zero in each half period.

B. Second example

Another example is given by the Langevin equation:

$$\dot{\theta} = V_0 k_0 \sin k_0\theta + f(t) + \sqrt{2D}\xi(t), \tag{13}$$

with the time-dependent potential function $\phi[\theta, f(t)] = [V_0 \cos k_0\theta - f(t)\theta]/D$. As it is not straightforward to evaluate the path integral $P^m(\theta_N t_N|\theta_0 t_0) = \int_{\theta_0}^{\theta_N + 2\pi m} \mathcal{D}\theta \exp - \int_{t_0}^{t_N} \{[\dot{\theta} - V_0 k_0 \sin k_0\theta - f(t)]^2/4D + V_0 k_0^2 \cos k_0\theta/2\}\, dt$, we use numerical simulations to obtain free energy. We plot the simulation results for the linear force protocol $f(t) = at$ in Fig. 3.

The simulations for Eq. (13) are verified by the following approximations in specific parameters regions, as shown in Fig. 3. First, when the potential height V_0 is large, the particle is trapped into the potential well, and the work becomes approximately $W \approx -\theta_0 \int_{t_0}^{t_N} dt\, \dot{f}/D$, where θ_0 is position of the minimum value in the potential well. As a result, free energy change $-\Delta\mathcal{F} \approx \theta_0 \int_{t_0}^{t_N} \dot{f} dt/D = a\theta_0 \Delta t/D$. Second, when V_0 is sufficiently small, we almost have the conservative potential flat as Eq. (8) in a short time region, and we can approximately use the analytic result from Eq. (8). The effect of the periodic potential accumulates when time goes on, and the simulation will eventually deviate from this approximation.

IV. DISCUSSION

The free energy changes obtained here can be tested in recent experimental systems such as the Brownian particle driven by a laser trap on a ring [3,4]. To experimentally prepare an initial equilibrium state of the system, we should stop the driving force and let the system relax for sufficient time. Within this period, the ensemble distribution on the line diffuses to infinity with approaching to zero everywhere. The distribution can then be treated as uniform on the ring, i.e., on an interval of real line with 2π length such as $[0,2\pi)$. Next, we vary the force to another value with measuring the work conducted in this process [24] and repeat the experiments for many times. Finally, we can obtain a converged value on the free energy change by Eq. (7).

The origins of the breakdown of detailed balance in the previous works [21,22,33–36] and here are different. The systems in Ref. [22] are with a natural boundary condition, and the breakdown of detailed balance is caused by a dynamical part with nonzero curl. In those systems, we can still successfully construct the potential function leading to the Boltzmann-Gibbs distribution, and then the free energy is defined by the partition function. In the present work, we discuss the system Eq. (1) with periodic boundary condition [2,3,10,37], and the nontrivial topology on a ring allows a current violating detailed balance. As a result, the steady state typically does not obey the Boltzmann-Gibbs distribution, and the free energy could no longer be obtained by the canonical ensemble.

Besides work, ensemble average for more thermodynamical variables can be calculated using Eq. (3) for systems with nontrivial topology, which can reveal richer thermodynamical information. For example, to quantify the energy dissipated into the environment, a kind of thermal energy can be obtained. For the example Eq. (8), from heat $Q = -\int_{t_0}^{t_N} dt\, \dot{\theta} f/D$, we get thermal energy $-\Delta\mathcal{T} = 2\int_{t_0}^{t_N} dt f^2/D$ (see details in the Appendices). This denotes the energy continuously put into the system in order to maintain the current as some thermal energy dissipates into the environment. The heat leads to the medium entropy production [2], and the thermal energy change corresponds to its ensemble average.

V. CONCLUSION

We have shown anomalous free energy changes by the nontrivial topology of the overdamped Langevin dynamics on a ring. We have demonstrated the anomalous behaviors in examples with both exact solutions and numerical simulations. The obtained free energy change is experimentally testable and can help to distinguish the degenerated steady states observed on the ring. The system Eq. (13) with periodic force can have richer phenomena including resonance. Future works also include conducting experiments to measure the energy changes calculated here and generalizing our treatment to a quantum regime.

ACKNOWLEDGMENTS

We thank Hong Qian, David Cai, Anthony J. Leggett, and Xiangjun Xing for the critical comments. This work is supported in part by the National 973 Project No. 2010CB529200 and by the Natural Science Foundation of China Projects No. NSFC61073087 and No. NSFC91029738.

APPENDIX A: DETAILED CALCULATION OF THE FIRST EXAMPLE

In this Appendix, we give detailed calculation of the first example [Eq. (8)]. Its time-dependent potential function is

$$\phi[\theta, f(t)] = -\frac{1}{D} f(t)\theta. \tag{A1}$$

1. Transition probability

The path integral for the winding number m is

$$P^m(\theta_N t_N|\theta_0 t_0) = \int_{\theta_0}^{\theta_N+2\pi m} \mathcal{D}\theta \times \exp\left\{-\int_{t_0}^{t_N} \frac{1}{4D}[\dot{\theta} - f(t)]^2\, dt\right\}. \tag{A2}$$

We solve it by the semiclassical method below. The action is

$$\mathbf{S} = \frac{1}{4D}\int_{t_0}^{t_N} [\dot{\theta} - f]^2\, dt. \tag{A3}$$

Its Lagrangian equation is

$$\ddot{\theta} - \dot{f} = 0, \tag{A4}$$

which leads to the solution

$$\theta(t) = \int_{t_0}^{t} f ds + At + B, \tag{A5}$$

where A and B are undetermined coefficients. By applying the boundary condition, we have

$$\theta_N = \int_{t_0}^{t_N} f ds + At_N + B, \quad \theta_0 = At_0 + B, \tag{A6}$$

which gives

$$A = \frac{\theta_N - \theta_0 - \int_{t_0}^{t_N} f ds}{\Delta t}, \qquad B = \frac{-\theta_N t_0 + \theta_0 t_N + t_0 \int_{t_0}^{t_N} f ds}{\Delta t}. \tag{A7}$$

Then the action of the classical path is

$$\mathbf{S} = \frac{1}{4D\Delta t}\left[\theta_N - \theta_0 - \int_{t_0}^{t_N} f dt\right]^2. \tag{A8}$$

Therefore, we have the transition probability for each winding number m:

$$P^m(\theta_N t_N|\theta_0 t_0) = \sqrt{\frac{1}{4\pi D\Delta t}} \exp\left\{-\frac{1}{4D\Delta t}\left[\theta_N + 2\pi m - \theta_0 - \int_{t_0}^{t_N} f(t) dt\right]^2\right\}. \tag{A9}$$

If choosing the initial distribution $\rho(\theta_0) = \delta(\theta - \theta_0)$, the probability in the winding number representation is

$$\begin{aligned} P(\theta_N t_N|t_0) &= \frac{1}{2\pi}\theta_3\left(-\frac{\theta_N - \int_{t_0}^{t_N} f(t)\, dt}{2}, \frac{iD\Delta t}{\pi}\right) \\ &= \frac{1}{2\pi}\sum_{m=-\infty}^{\infty} e^{-D\Delta t m^2 - im[\theta_N - \int_{t_0}^{t_N} f(t)\, dt]} \\ &\to \frac{1}{2\pi} \end{aligned} \tag{A10}$$

when $t_N \to \infty$.

2. Free energy

Next, we consider the process of varying control parameters from time t_0 to time t_N. The work is

$$W = -\frac{1}{D}\int_{t_0}^{t_N} dt\ \dot{f}\theta. \tag{A11}$$

The weighting propagator for the work $\langle e^{-W}\rangle_{\rm PD}$ with winding number m is

$$P_W^m(\theta_N t_N|\theta_0 t_0) = \int_{\theta_0}^{\theta_N+2\pi m} \mathcal{D}\theta \exp\left\{-\int_{t_0}^{t_N}\frac{[\dot{\theta}-f(t)]^2}{4D}\,dt + \frac{1}{D}\int_{t_0}^{t_N} dt\ \dot{f}\theta\right\}, \tag{A12}$$

which can be calculated out explicitly by the similar method as above. We obtain the weighting propagator with winding number m:

$$P_W^m(\theta_N t_N|\theta_0 t_0) = \sqrt{\frac{1}{4\pi D\Delta t}}\exp -\frac{1}{4D\Delta t}\left\{\left[\theta_N + 2\pi m - \theta_0 + \int_{t_0}^{t_N} f dt\right]^2 - 4\Delta t[f(t_N)(\theta_N+2\pi m) - f(t_0)\theta_0]\right\}. \tag{A13}$$

We let the initial state obey the distribution $\rho(\theta_0,t_0) = 1/2\pi$ on $[0,2\pi)$ and get

$$\begin{aligned}\langle e^{-W}\rangle_{\rm PD} &= \int_0^{2\pi} d\theta_N \sum_{m=-\infty}^{\infty}\int_0^{2\pi} d\theta_0 P_{ss}(\theta_0,t_0)P_W^m(\theta_N t_N|\theta_0 t_0)\\ &= \int_0^{2\pi} d\theta_0 \frac{1}{2\pi}\int_{-\infty}^{\infty} d\theta_N \sqrt{\frac{1}{4\pi D\Delta t}}\exp -\frac{1}{4D\Delta t}\left\{\left[\theta_N - \theta_0 + \int_{t_0}^{t_N} f dt\right]^2 - 4\Delta t[f(t_N)\theta_N - f(t_0)\theta_0]\right\}\\ &= \frac{D\{e^{2\pi[f(t_N)-f(t_0)]/D}-1\}}{2\pi[f(t_N)-f(t_0)]}\exp\frac{1}{D}f(t_N)\left[\Delta t f(t_N) - \int_{t_0}^{t_N} f dt\right].\end{aligned} \tag{A14}$$

3. Thermal energy

We can also calculate the ensemble average of the heat:

$$Q \doteq -\frac{1}{D}\int_{t_0}^{t_N} dt\,\dot{\theta} f, \tag{A15}$$

and the weighting propagator for the heat $\langle e^{-Q}\rangle_{\rm PD}$ with winding number m is

$$P_Q^m(\theta_N t_N|\theta_0 t_0) = \int_{\theta_0}^{\theta_N+2\pi m}\mathcal{D}\theta\exp\left\{-\int_{t_0}^{t_N}\frac{[\dot{\theta}-f(t)]^2}{4D}\,dt + \frac{1}{D}\int_{t_0}^{t_N} dt\,\dot{\theta} f\right\}. \tag{A16}$$

Similarly, by the semiclassical method, we obtain

$$P_Q^m(\theta_N t_N|\theta_0 t_0) = \sqrt{\frac{1}{4\pi D\Delta t}}\exp -\frac{1}{4D\Delta t}\left\{\left[\theta_N + 2\pi m - \theta_0 - 3\int_{t_0}^{t_N} f dt\right]^2 - 8\Delta t\int_{t_0}^{t_N} dt f^2\right\}. \tag{A17}$$

Let the initial state obey the distribution $\rho(\theta_0,t_0) = 1/2\pi$ on $[0,2\pi)$, and

$$\langle e^{-Q}\rangle_{\rm PD} = \int_0^{2\pi} d\theta_N \sum_{m=-\infty}^{\infty}\int_0^{2\pi} d\theta_0 P_{ss}(\theta_0,t_0)P_Q^m(\theta_N t_N|\theta_0 t_0) = \exp\left\{\frac{2}{D}\int_{t_0}^{t_N} dt f^2\right\}. \tag{A18}$$

4. Different force protocols

For some special protocols of $f(t)$, we have the following:

(1) When $f(t) = f_0$ being a constant,

$$\langle e^{-W}\rangle_{\rm PD} = 1, \tag{A19}$$

$$\langle e^{-Q}\rangle_{\rm PD} = \exp\left\{\frac{2}{D}f_0^2\Delta t\right\}. \tag{A20}$$

(2) When $f(t)$ is a step function with strength Δf starting at t_0, $\dot{f} = \Delta f\delta(t_0)$, and

$$\langle e^{-W}\rangle_{\rm PD} = \frac{D\{e^{2\pi\Delta f/D}-1\}}{2\pi\Delta f}, \tag{A21}$$

$$\langle e^{-Q}\rangle_{\rm PD} = \exp\left\{\frac{2}{D}(\Delta f)^2\Delta t\right\}. \tag{A22}$$

(3) When $f(t) = at$ is linear function with $f(t_0) = 0$, $\dot{f} = a$, and

$$\langle e^{-W}\rangle_{\rm PD} = \frac{D\{e^{2\pi a\Delta t/D} - 1\}}{2\pi a\Delta t}\exp\left[\frac{1}{2D}a^2 t_N(\Delta t)^2\right], \tag{A23}$$

$$\langle e^{-Q}\rangle_{\rm PD} = \exp\left\{\frac{2a^2}{D}\frac{t_N^3 - t_0^3}{3}\right\}. \tag{A24}$$

(4) When $f(t) = \sin\omega t$, $\dot{f}(t) = \omega\cos\omega t$, and

$$\langle e^{-W}\rangle_{\rm PD} = \frac{D\{e^{2\pi[\sin\omega t_N - \sin\omega t_0]/D} - 1\}}{2\pi[\sin\omega t_N - \sin\omega t_0]}\exp\left\{\frac{1}{D}\sin\omega t_N\left[\Delta t\sin\omega t_N - \frac{1}{\omega}(\cos\omega t_0 - \cos\omega t_N)\right]\right\}, \tag{A25}$$

$$\langle e^{-Q}\rangle_{\rm PD} = \exp\left\{\frac{1}{D}\left[\Delta t - \frac{1}{2\omega}(\sin 2\omega t_N - \sin 2\omega t_0)\right]\right\}. \tag{A26}$$

If $t_N - t_0 = 2\pi n/\omega (n \in Z^+)$ and $t_N = m\pi/\omega (m \in Z^+)$, then $\langle e^{-W}\rangle_{\rm PD} = 1$ and the free energy equals zero. The free energy and the thermal energy are equal to each other when $\sin\omega t_N - \sin\omega t_0 = 0$ and $t_N = (2m-1)\pi/2\omega (m \in Z^+)$.

5. Free energy with different initial distributions

In the last subsection, we calculated the ensemble value by using the initial distribution on $[0,2\pi)$. Here we demonstrate that the result is different if we choose other initial distributions. In general, different initial distribution (including the uniform distribution with different intervals on real line) leads to distinct results of free energy, which is a consequence of applying the washboard potential. The choice of distribution depends on how to implement the initial state in real experiments.

First, we consider the uniform distribution on $[-\pi,\pi)$ initially, and get

$$\begin{aligned}\langle e^{-W}\rangle_{\rm PD} &= \int_{-\pi}^{\pi} d\theta_0\frac{1}{2\pi}\exp\frac{1}{D}\left\{\theta_0[f(t_N) - f(t_0)] - f(t_N)\int_{t_0}^{t_N} f dt + \Delta t f^2(t_N)\right\}\\ &= \frac{D\{e^{\pi[f(t_N)-f(t_0)]/D} - e^{-\pi[f(t_N)-f(t_0)]/D}\}}{2\pi[f(t_N) - f(t_0)]}\exp\frac{1}{D}f(t_N)\left[\Delta t f(t_N) - \int_{t_0}^{t_N} f\,dt\right].\end{aligned} \tag{A27}$$

For the force $f(t) = \sin\omega t$, we obtain

$$\langle e^{-W}\rangle_{\rm PD} = \frac{D\{e^{\pi[\sin\omega t_N - \sin\omega t_0]/D} - e^{-\pi[\sin\omega t_N - \sin\omega t_0]/D}\}}{2\pi[\sin\omega t_N - \sin\omega t_0]}\exp\frac{1}{D}\sin\omega t_N\left[\Delta t\sin\omega t_N - \frac{1}{\omega}(\cos\omega t_0 - \cos\omega t_N)\right]. \tag{A28}$$

Note that for $t = \pi/2$ and $t = 3\pi/2$ (with $t_0 = 0$), the maximums of free energy change are now equal to each other. Thus, the consecutive two peaks of free energy, e.g., $t = \pi/2$ and $t = 3\pi/2$, have the same height, different from that shown in Fig. 2, where we use the result with the initial distribution on $[0,2\pi)$.

Second, we consider the delta distribution $P_{ss}(\theta_0,t_0) = \delta(\theta_0)$ initially and get

$$\begin{aligned}\langle e^{-W}\rangle_{\rm PD} &= \int_{-\infty}^{\infty} d\theta_0\delta(\theta_0)\exp\frac{1}{D}\left\{\theta_0[f(t_N) - f(t_0)] - f(t_N)\int_{t_0}^{t_N} f dt + \Delta t f^2(t_N)\right\}\\ &= \exp\frac{1}{D}f(t_N)\left[\Delta t f(t_N) - \int_{t_0}^{t_N} f\,dt\right].\end{aligned} \tag{A29}$$

For the force $f(t) = \sin\omega t$, we obtain

$$\langle e^{-W}\rangle_{\rm PD} = \exp\frac{1}{D}\sin\omega t_N\left[\Delta t\sin\omega t_N - \frac{1}{\omega}(\cos\omega t_0 - \cos\omega t_N)\right]. \tag{A30}$$

6. Numerical simulation

The Langevin equation in the difference form is

$$d\theta = f(t)\,dt + \sqrt{2D}dW(t). \tag{A31}$$

Starting from a delta distribution $\delta(\theta_0)$ at time $t_0 = 0$, we can sample Eq. (A31) with $f(t) = 0$ for sufficiently long time and get a normalized steady state distribution $P_{ss}(\theta)$. The path ensemble for the work can be sampled by

$$\langle e^{-W}\rangle_{\rm PD} = \sum_{\theta(t_0)\in P_{ss}(\theta)}\sum_{\rm path}\exp\left[\frac{1}{D}\sum_{n=0}^{N}\dot{f}(t_n)\theta(t_n)\,dt\right], \tag{A32}$$

where P_{ss} is the steady state distribution, and dt is small time slice.

Similarly, the path ensemble for the heat is

$$\langle e^{-Q}\rangle_{\rm PD} = \sum_{\theta(t_0)\in P_{ss}(\theta)} \sum_{\rm path} \exp\left[\frac{1}{D}\sum_{n=0}^{N} \dot{\theta}(t_n) f(t_n)\, dt\right]. \quad \text{(A33)}$$

For simulations, we consider the following force protocols:

(1) $f(t) = at$ is linear function with $f(t_0) = 0$, $\dot{f} = a$.

(2) $f(t) = \sin \omega t$, and $\dot{f}(t) = \omega \cos \omega t$.

The case with $f(t) = \Delta f \theta(t)$ is straightforward for simulation and thus is not plotted.

In simulations, we use θ as a variable in $(-\infty,\infty)$, and does not restrict it in $[0,2\pi)$, because the particle is treated as moving in a washboard potential with $\theta \in (-\infty,\infty)$. Then one may wonder what is the difference of simulating Eq. (1) on a ring and on the real line $\mathcal{R}$. The topological property of the ring space is reflected by (1) the initial distribution used in simulation is set on the ring $[0,2\pi)$; (2) to get the evolved distribution on the ring, we resum up the distribution pieces on the real line with modulo of 2π. By this procedure, for example, the steady state distribution for Eq. (8) is always uniform on the ring, while the probability distribution for Eq. (8) on the real line is approaching zero everywhere. When doing analytical calculations, we treat θ as a variable in $[0,2\pi)$ explicitly and then include all the possible stochastic paths in the operation process during $\Delta t = t_N - t_0$ by counting different winding numbers and finally integrating $\theta_N \in [0,2\pi)$. These different treatments on θ in the numerical and analytic methods are essentially the same, because they both count all configurations in the path ensemble. They also lead to consistent results, as verified in Fig. 3.

APPENDIX B: DETAILED CALCULATION OF THE SECOND EXAMPLE

In this Appendix, we give detailed calculation of the second example [Eq. (13)]. The time-dependent potential function is

$$\phi[\theta, f(t)] = \frac{1}{D}[V_0 \cos k_0\theta - f(t)\theta]. \quad \text{(B1)}$$

The steady state does not obey the Boltzmann-Gibbs distribution when the force performs [38]. As it is not straightforward to obtain an explicit formula by solving the path integral of this example, we use numerical samplings to simulate the free energy differences.

Numerical simulation

The Langevin equation in the difference form is

$$d\theta = V_0 k_0 \sin k_0\theta\, dt + f(t)\, dt + \sqrt{2D} dW(t). \quad \text{(B2)}$$

The path ensemble for the work is

$$\langle e^{-W}\rangle_{\rm PD} = \sum_{\theta(t_0)\in P_{ss}(\theta)} \sum_{\rm path} \exp\left[\frac{1}{D}\sum_{n=0}^{N} \dot{f}(t_n)\theta(t_n)\, dt\right], \quad \text{(B3)}$$

where P_{ss} is the steady state distribution:

$$P_{ss}(\theta_0) = \frac{1}{Z}\exp\left(-\frac{1}{D}V_0 \cos k_0\theta_0\right), \quad \text{(B4)}$$

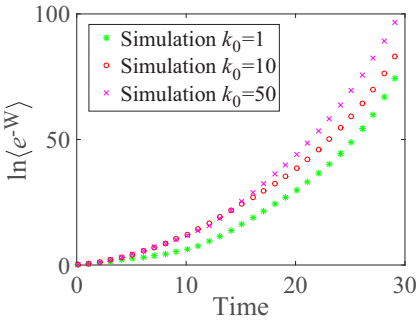

FIG. 4. (Color online) Free energy of the example Eq. (13) with linear force protocol $f(t) = at$ are simulated. We consider three different values of k_0 for free energy: $k_0 = 1$, $k_0 = 10$, and $k_0 = 50$. The other parameters are $t_0 = 0$, $D = 1$, $V = 5$, and $a = 0.16$.

with the partition function:

$$Z = \int_0^{2\pi} d\theta_0 \exp\left(-\frac{1}{D}V_0 \cos k_0\theta_0\right). \quad \text{(B5)}$$

Similarly, the path ensemble for the heat is

$$\langle e^{-Q}\rangle_{\rm PD} = \sum_{\theta(t_0)\in P_{ss}(\theta)} \sum_{\rm path} \exp\left[\frac{1}{D}\sum_{n=0}^{N} \dot{\theta}(t_n) \times [V_0 k_0 \sin k_0\theta(t_n) + f(t_n)]\, dt\right]. \quad \text{(B6)}$$

Besides the figures in the main text, here we also simulate free energy and thermal energy for different values of k_0 in Eq. (13), as shown in Figs. 4 and 5.

We consider the force protocol $f(t) = at$ with $\dot{f} = a$ in time interval $[0,t_N]$. We have the following approximation: When t is very small, $f(t)$ in Eq. (13) can be neglected. Then the particle will soon be trapped in the wells of the potential ϕ. Thus, θ is a constant under the ensemble average. In our simulation, we let $k_0 = D = 1$, and thus the potential well is at $\theta = \pi$. As a result, the free energy change $\Delta\mathcal{F} \approx \pi \int_{t_0}^{t_N} \dot{f} dt = a\pi\Delta t$.

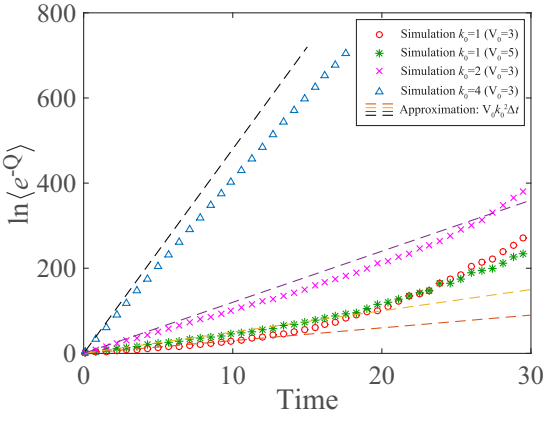

FIG. 5. (Color online) Thermal energy of the example [Eq. (13)] with linear force protocol $f(t) = at$ are simulated. We consider three different values of k_0 for thermal energy: $k_0 = 1$, $k_0 = 2$, and $k_0 = 4$. The other parameters are $t_0 = 0$, $D = 1$, $V = 3(5)$, and $a = 0.16$.

For the thermal energy, we have approximately

$$\langle e^{-Q}\rangle_{\rm PD} \approx \sum_{\theta(t_0)\in P_{ss}(\theta)} \sum_{\rm path} \times \exp\left[\frac{1}{D}\int_{\theta(t_0)}^{\theta(t_N)} V_0 k_0 \sin(k_0\theta)\, d\theta\right], \quad \text{(B7)}$$

since the term $f(t_n)d\theta(t_n) \approx 0$ as $\theta(t_n)$ is constant. Notice that when doing numerical simulation, we used the pre-point in each interval, which corresponds to Ito's calculus. Thus, we should apply Ito's formula [19]: for a smooth function $A(\theta(t))$ with θ obeying the stochastic differential equation (1),

$$dA(\theta) \approx A'(\theta)\, d\theta + \tfrac{1}{2}A''(\theta) 2D\, dt, \quad \text{(B8)}$$

to the order of dt. Then we get the integral form:

$$A(\theta(t))|_{t_0}^{t_N} \approx \int_{\theta(t_0)}^{\theta(t_N)} A'(\theta)\, d\theta + \int_{t_0}^{t_N} A''(\theta) D\, dt. \quad \text{(B9)}$$

We let $A(\theta) = \cos(k_0\theta)$ and have

$$\begin{aligned}\frac{1}{D}\int_{\theta(t_0)}^{\theta(t_N)} & V_0 k_0 \sin(k_0\theta)\, d\theta \\ &\approx \frac{1}{D} V_0 k_0 \left\{ -\frac{1}{k_0}[\cos k_0\theta(t_N) - \cos k_0\theta(t_0)] \right. \\ &\quad \left. - k_0 D\Delta t \cos k_0\theta(t_N) \right\} \\ &\approx -V_0 k_0^2 \Delta t \cos k_0\theta(t_N), \end{aligned} \quad \text{(B10)}$$

where we use the approximation that $\theta(t_n)$ and $\cos k_0\theta(t_N)$ are constant. As a result, the thermal energy difference is a linear function of time t with slope $V_0 k_0^2$.

When t is sufficiently large, $f(t)$ is dominate in Eq. (13). Then the free and thermal energy change of the system behaves like the first example [Eq. (8)].

In the time region between the above two, we use $\partial_\theta \phi = -[V_0 k_0 \sin k_0\theta + f(t)]/D$ and get that the potential wells will disappear when $f(t) \geqslant V_0 k_0$. Thus, we have approximately that the crossover of the above two cases happens at the time $t \approx V_0 k_0/a$.

[1] P. Nelson, *Biological Physics: Energy, Information, Life* (Freeman, New York, 2004).
[2] T. Hatano and S.-I. Sasa, Phys. Rev. Lett. **86**, 3463 (2001).
[3] U. Seifert, Rep. Prog. Phys. **75**, 126001 (2012).
[4] J. R. Gomez-Solano, A. Petrosyan, S. Ciliberto, R. Chetrite, and K. Gawedzki, Phys. Rev. Lett. **103**, 040601 (2009).
[5] C. Van den Broeck and M. Esposito, Phys. Rev. E **82**, 011144 (2010).
[6] H. Gang, A. Daffertshofer, and H. Haken, Phys. Rev. Lett. **76**, 4874 (1996).
[7] P. Reimann, C. Van den Broeck, H. Linke, P. Hänggi, J. M. Rubi, and A. Pérez-Madrid, Phys. Rev. Lett. **87**, 010602 (2001).
[8] X.-G. Ma, P.-Y. Lai, B. J. Ackerson, and P. Tong, Phys. Rev. E **91**, 042306 (2015).
[9] R. Hayashi, K. Sasaki, S. Nakamura, S. Kudo, Y. Inoue, H. Noji, and K. Hayashi, Phys. Rev. Lett. **114**, 248101 (2015).
[10] M. Esposito and C. Van den Broeck, Phys. Rev. Lett. **104**, 090601 (2010).
[11] H. Ge, M. Qian, and H. Qian, Phys. Rep. **510**, 87 (2012).
[12] Edited by R. Klages, W. Just, and C. Jarzynski, *Nonequilibrium Statistical Physics of Small Systems: Fluctuation Relations and Beyond* (Wiley-VCH, New York, 2013).
[13] J. Prost, J.-F. Joanny, and J. M. R. Parrondo, Phys. Rev. Lett. **103**, 090601 (2009).
[14] P. Hänggi and F. Marchesoni, Rev. Mod. Phys. **81**, 387 (2009).
[15] K. Hayashi, H. Ueno, R. Iino, and H. Noji, Phys. Rev. Lett. **104**, 218103 (2010).
[16] R. P. Feynman, R. B. Leighton, and M. Sands, *The Feynman Lectures on Physics, Vol. 3* (Addison-Wesley, New York, 1964).
[17] A. O. Caldeira and A. J. Leggett, Ann. Phys. **149**, 374 (1983).
[18] Y. Tang, R. Yuan, and P. Ao, Phys. Rev. E **89**, 062112 (2014).
[19] C. W. Gardiner, *Handbook of Stochastic Methods* (Springer, Berlin, 2004).
[20] L. Schulman, *Techniques and Applications of Path Integration*, Vol. 140 (Wiley, New York, 1981).
[21] P. Ao, Commun. Theor. Phys. **49**, 1073 (2008).
[22] Y. Tang, R. Yuan, J. Chen, and P. Ao, Phys. Rev. E **91**, 042108 (2015).
[23] C. Jarzynski, Phys. Rev. Lett. **78**, 2690 (1997).
[24] J. Liphardt, S. Dumont, S. B. Smith, I. Tinoco, and C. Bustamante, Science **296**, 1832 (2002).
[25] P. Ao and J. Rammer, Superlattices Microstruct. **11**, 265 (1992).
[26] M. Chaichian and A. Demichev, *Stochastic Processes and Quantum Mechanics, Path Integrals in Physics*, Vol. I (IOP, Bristol, 2001).
[27] Y. Tang, R. Yuan, and P. Ao, J. Chem. Phys. **141**, 044125 (2014).
[28] M. Campisi, P. Hänggi, and P. Talkner, Rev. Mod. Phys. **83**, 771 (2011).
[29] A. M. Jayannavar and M. Sahoo, Phys. Rev. E **75**, 032102 (2007).
[30] G. Hummer and A. Szabo, Proc. Natl. Acad. Sci. USA **98**, 3658 (2001).
[31] C. Jarzynski, J. Stat. Mech. (2004) P09005.
[32] F. W. J. Olver, D. W. Lozier, R. F. Boisvert, and C. W. Clark, *NIST Handbook of Mathematical Functions* (Cambridge University Press, New York, 2010).
[33] P. Ao, J. Phys. A **37**, L25 (2004).
[34] C. Kwon, P. Ao, and D. J. Thouless, Proc. Natl. Acad. Sci. USA 102, 13029 (2005).
[35] V. Y. Chernyak, M. Chertkov, and C. Jarzynski, J. Stat. Mech. (2006) P08001.
[36] C. Kwon, J. D. Noh, and H. Park, Phys. Rev. E **83**, 061145 (2011).
[37] R. A. Blythe and M. R. Evans, J. Phys. A **40**, R333 (2007).
[38] H. Risken, *The Fokker-Planck Equation: Methods of Solution and Applications*, Vol. 18 (Springer, New York, 1996).